

RESEARCH ARTICLE

 OPEN ACCESS

Received: 14-12-2021

Accepted: 03-08-2022

Published: 27-08-2022

Citation: Thepsri N, Kaewsrichan J (2022) Evaluation of Alkaline-Treated Polycaprolactone and Zr-Hydroxyapatite as a Drug Delivery System in Dentistry. Indian Journal of Science and Technology 15(33): 1624-1633. <https://doi.org/10.17485/IJST/v15i33.2336>

* Corresponding author.

jasadee.k@psu.ac.th

Funding: Funding of this project was supported by The Graduate School at Prince of Songkla University (PSU), Drug Delivery System Excellence Center, and Faculty of Pharmaceutical Sciences, PSU, Hat-Yai, Songkhla, Thailand.

Competing Interests: None

Copyright: © 2022 Thepsri & Kaewsrichan. This is an open access article distributed under the terms of the [Creative Commons Attribution License](#), which permits unrestricted use, distribution, and reproduction in any medium, provided the original author and source are credited.

Published By Indian Society for Education and Environment ([iSee](#))

ISSN

Print: 0974-6846

Electronic: 0974-5645

Evaluation of Alkaline-Treated Polycaprolactone and Zr-Hydroxyapatite as a Drug Delivery System in Dentistry

Nicha Thepsri¹, Jasadee Kaewsrichan^{1*}

¹ Department of Pharmaceutical Chemistry and Drug Delivery System Excellence Center, Faculty of Pharmaceutical Sciences, Prince of Songkla University, Hat-yai, Songkhla, 90112, Thailand

Abstract

Objectives: To develop alkaline-treated polycaprolactone (PCL) and Zr-hydroxyapatite (Zr-HA) and fabricate their mixtures as drug delivery systems for dental application. **Methods:** PCL was subjected to hydrolysis by using concentrated NaOH. Zr-HA was synthesized by co-precipitation reaction that contained $\text{Ca}(\text{NO}_3)_2$, $(\text{NH}_4)_2\text{HPO}_4$ and ZrO_2 at 65°C . The obtained materials were characterized by using techniques such as X-Ray Fluorescence, Fourier Transform Infrared Spectroscopy, X-Ray Diffraction, or rheometric analysis. Various compositions of the Zr-HA and the modified-PCL were used for preparing drug delivery systems, and properties including cytotoxicity, degradation, and toluidine blue (TB) binding/releasing were investigated. **Findings:** The synthesized Zr-HA was more non-stoichiometric than HA-control. Improved hydrophilicity was evident for the modified-PCL. Drug carriers composing of the Zr-HA and the modified-PCL were increasingly degradable in phosphate buffer saline solution compared to those containing HA/PCL-control, resulting in 9% and 6% weight loss after 8 weeks of the immersion, respectively. Binding of TB on the Zr-HA/the modified-PCL mixture increased while the release of such bound dye decreased in comparison with that of HA/PCL counterpart. All of the developed materials were non-cytotoxic based on MTT assay using L929 cell line. **Novelty:** Partial inclusion of Zr^{4+} ions in Ca^{2+} lattices of HA resulted in fairly degradable Zr-HA. Shortening the epsilon-caprolactone units of PCL by strong bases was simple in producing fragmented PCL polymer that exhibited improvement of hydrophilic interaction towards another. Varying the weight ratios of the Zr-HA and the modified-PCL when to prepare drug carriers is possible to acquire optimal binding/releasing profiles of drugs in dental cavities.

Keywords: Dental ceramic; hydroxyapatite; polycaprolactone; surface hydrophilicity; drug delivery system

1 Introduction

Dental and periodontal care in restorative dentistry is superior when using biocompatible and biodegradable drug delivery systems to eradicate bacterial infection, restore wound, and guide bone regeneration because re-operation will not be carried out⁽¹⁾ and drug bioavailability will be boosted by the limited diffusion and degradation of the loaded drugs⁽²⁾. Osseous tissues including teeth are mainly constituted by ions of calcium (Ca^{2+}) and phosphate (PO_4^{3-}) in a form of hydroxyapatite (HA). Indeed, native HA is structurally non-stoichiometric because trace cations such as Na^+ , K^+ , Mg^{2+} , Sr^{2+} , Zn^{2+} , and Al^{3+} and anionic species like F^- , Cl^- , SO_4^{2-} , and CO_3^{2-} are included in HA molecular lattices. These ionic inclusions are determined to associate the strength and the regeneration capacity of bones⁽³⁾. Several types of non-stoichiometric HA have been prepared in laboratories for various purposes. For example, zirconia doped HA has shown lowered degree of crystallinity in accompany with hardness decrement⁽⁴⁾. Co-substitution of Zr^{4+} and Ce^{3+} ions in the molecular lattices of HA and Fluoro-HA has exhibited a positive consequence on their toughness⁽⁵⁾. Insertion of Sr^{2+} in HA lattices has been inductive for apatite formation and mineralization⁽⁶⁾. Previously, HA has been used in restorative procedures as bone cement for increasing bone fixation⁽⁷⁾. Furthermore, this ceramic has been speculated as a suitable niche for drug loading in drug delivery systems due to the properties like high porosity and great binding affinity⁽⁸⁾. It might be used as a durable support in severe damaged bones as well because insignificant amount of HA (~1-2%) is degraded in physiologic environment per year⁽⁹⁾. However, HA has different drawbacks that limit its applications, such as poor compressive strength, low toughness, and inferior elasticity. Interestingly, such the deficiencies have been improved for example by including biodegradable polymers such as polylactic acid, to result in composites suitable for restorative maxillofacial surgery⁽¹⁰⁾. Polycaprolactone (PCL) is a familiar biodegradable polymer in bone tissue engineering/regeneration. However, the polymer is fairly hydrophobic that is restrictive for water adsorption and cell adhesion, consequently leading to biologically inactive. Incorporation of HA into PCL has exhibited improvement of the polymer's bioactivity^(11,12). In this research, another non-stoichiometric Zr-HA was synthesized in that Ca^{2+} ions were competitively substituted by Zr^{4+} ions while co-precipitated to form HA. Thin-film of PCL was produced before to be incubated with concentrated NaOH to accelerate the rate of alkaline hydrolysis. Material characterizations were performed by using techniques such as X-Ray Diffraction (XRD), X-Ray Fluorescence (XRF), Fourier Transform Infrared Spectroscopy (FTIR), or rheometric analysis. Drug delivery fillers containing different weight ratios of the Zr-HA and the modified-PCL were prepared. This was followed by the determination of cytotoxicity, degradability, and binding/releasing property using TB as a model drug. Results acquired would be valuable towards subsequent researches in developing drug delivery systems for extemporaneous use in maxillofacial surgery and restorative dentistry.

2 Methodology

2.1 Materials

All the used chemicals were of analytical grade. Chloroform and sodium chloride (NaCl) were acquired from RCI Labscan Limited (Bangkok, Thailand). Toluidine blue was obtained from Fluka (Buch's, Switzerland). Polycaprolactone (MW ~14,000 Da), diammonium hydrogen phosphate ($(\text{NH}_4)_2\text{HPO}_4$), sodium bicarbonate (NaHCO_3), potassium chloride (KCl), and acetic acid were purchased from Sigma-Aldrich Corporation (Missouri, USA). Calcium nitrate tetrahydrate ($\text{Ca}(\text{NO}_3)_2 \cdot 4\text{H}_2\text{O}$) and zirconium oxide (ZrO_2) were obtained from Riedel-de Haën (North Carolina, US). Nitric acid (HNO_3), hydrochloric acid (HCl), ethanol, and potassium dihydrogen phosphate (KH_2PO_4) were acquired from Merck (Darmstadt, Germany). Ammonia solution (25%) was bought from LobaChemie (Mumbai, India).

2.2 Synthesis of Zr-HA

To synthesize Zr-HA, our previously described method was adopted⁽¹³⁾. In brief, 100 mL of 0.6 M $(\text{NH}_4)_2\text{HPO}_4$ solution were gradually added into a beaker containing 100 mL of 1.0 M $\text{Ca}(\text{NO}_3)_2 \cdot 4\text{H}_2\text{O}$ at 65°C with gentle stirring. By theory, 0.1 mole HA is formed using these rigorous reactants. Next, ZrO_2 weighing equivalent to 0.01 or 0.05 mole was added while stirring. Concentrated nitric acid was gradually added until clear solution was obtained. The reaction pH was adjusted to pH 11 by using 25% ammonia and aged overnight at room temperature with continuous stirring. The formed precipitate was filtered through Whatman filter paper No. 42 and washed several times with DI water. The filtered powder was dried at 80°C in a hot-air oven, followed by sintering at 1150°C for 4 h in the air. The sintered powder was soaked in phosphate buffer saline solution (PBS) for 14 days before removal. Excess PBS was completely washed out by using DI water. The resulting Zr-HA was dried at 80°C and ground to fine powder by using a ball mill machine (HSM 100H, Herzog GmbH, Germany). Two Zr-HA products were obtained, namely 0.1Zr-HA or 0.5Zr-HA, depending on the number of moles of ZrO_2 being added. They were kept in close

containers at room temperature until use.

2.3 Production of the modified-PCL

A solution of 50% w/v PCL in chloroform was prepared. Five milliliters of this solution were poured onto a glass Petri dish and left overnight in a fume hood. After that thin film of PCL was formed. Excess volume of NaOH solution, 3M or 5M, was poured on top to completely cover the film for 6 h. Then, the base solution was drained off, and the film was washed several times by using DI water until the pH of the washed water getting neutral. The alkaline-treated film was dried in the air and ground to fine powder using a mortar. Two types of the modified-PCL were developed, namely 3M-PCL or 5M-PCL, depending on NaOH concentration being used for the incubation. They were kept in well-close containers at room temperature until use.

2.4 Preparation of the Zr-HA/the modified-PCL composites

Composites that contained the Zr-HA and the modified-PCL at 1:2 and 2:1 w/w ratios were prepared. Briefly, the modified-PCL powder was completely reconstituted in chloroform in a tube into which the Zr-HA powder was gradually added. The tube was gently rolled until homogeneous paste was acquired. The paste was air-dried for 3 days in a fume hood and ground to be fine grain using a mortar. The resulting composite was kept in a close container until use.

2.5 Material characterizations

2.5.1 XRF of the Zr-HA

The XRF spectrometer (PW 2400, PHILIPS PANalytical, The Netherlands) was used for determination of H, C, N, O, Ca, P, and Zr that would present in the synthesized Zr-HA. The instrument was operated at 3 kW in a 1 Pa vacuum chamber to prevent artifacts from the air. The 2θ range of 0-100 mrad ($0 - 6^\circ$) was recorded.

2.5.2 FTIR of the modified-PCL

A KBr dish containing an equal weight of the modified-PCL and potassium bromide was prepared by using a suitable pressing apparatus. FTIR spectra were recorded by using the FTIR spectrometer (Perkin-Elmer, USA) within a wavelength range of 4400 - 450 cm^{-1} at 8 cm^{-1} resolutions.

2.5.3 Viscosity of the modified-PCL

Five grams of the modified-PCL were dissolved in 10 mL chloroform to produce 50% w/v solution, which was measured for the viscosity at room temperature using the rotational rheometer (DV-IIITM Ultra, BROOKFIELD, USA) according to the instrument's guidelines.

2.5.4 XRD of the prepared composites

The X-Ray diffractometer (XRD, PHILIPS X'Pert MPD, The Netherlands) was used for recording XRD profiles. The instrument was operated using Cu $K\alpha$ radiation ($\lambda=1.54060 \text{ \AA}$) at a voltage of 40 KV. The 2θ range of 5.0 and 90.0 $^\circ$ was conducted by scanning with an incident angle of 0.2 $^\circ$ and an increasing rate of 2.4 $^\circ$ per minute.

2.5.5 Scanning Electron Microscopy (SEM)

The scanning electron microscope (Quanta 400; FEI, Brno, Czech Republic) was used for determining surface morphologies of the mixed composites after gold coating.

2.6 In vitro degradation

A test sample was weighed to obtain an original weight (W_0). This weighed sample was immersed in PBS for a time period of 8 weeks at room temperature. Such the immersed sample was removed at a certain time duration, washed several times by using distilled water, air-dried for 4 h, and then freeze-dried. The dried sample was weighed again and the weight was recorded as W_n (where $n = 1, 2, \dots$, or 8 weeks of the immersed duration). The % degradation was calculated by using the equation below:

$$\% \text{ Degradation} = \frac{W_0 - W_n}{W_0} \times 100$$

2.7 Binding and releasing of TB to and from the composites

TB was used as a model drug in binding/releasing assays because various affinities were speculated to involve the TB binding, such as dipole-dipole, charged-charged, and hydrophobic/plan interactions. Furthermore, it was simple to quantify the amount of the dye that bound to or released from test specimens by measuring the OD₆₃₀ of the dye solution under investigated. In brief, TB solution at a concentration of 0.4 mg mL⁻¹ in water was prepared and measured for the OD₆₃₀ (A₀). A test sample was added into a tube containing 1 mL of the dye solution and left for 24 h at room temperature. Then, the OD₆₃₀ of the supernatant was recorded (A₁). The %TB binding was calculated by using the equation as follows:

$$\% \text{ TB binding} = \frac{A_0 - A_1}{A_0} \times 100$$

To draw the corresponding release profile, such immersed sample was taken out from the tube. Excess dye was removed by washing several times with distilled water and placed it on an absorbent paper to remove excess water. After that it was immersed in another tube containing 5 mL of PBS. Release test was carried out at 37°C for 120 h during which the supernatant was taken out for measuring the OD₆₃₀. The % TB release was calculated by comparing with the TB standard curve.

2.8 Cytotoxicity of the composites

A test composite was immersed in 2 mL of PBS for 24 h at room temperature with gentle shaking. The supernatant was filtered through a 0.22- μ m syringe filter and used as a test solution. Mouse fibroblast cell line L929 (ATCC) was kindly obtained from Prof. Teerapol Srichana (Faculty of Pharmaceutical Sciences, Prince of Songkla University, Thailand). The cells were routinely grown in Minimum Essential Medium alpha (MEM- α) supplemented with 10% fetal bovine serum, 100 units mL⁻¹ penicillin and 100 μ g mL⁻¹ streptomycin in a 5% CO₂ incubator at 37°C. The medium was changed every 3 days. MTT method was applied for cytotoxic measurement according to the previous literature⁽¹⁴⁾. Briefly, ~90% confluence of the cell monolayer in a well of 96-wells plate was prepared. The medium was removed immediately before testing. A mixture of 120 μ L of MEM- α and 50 μ L of a test solution was added into each well, and the cells were incubated in the incubator for 24 h at 37°C. After the medium was withdrawn, 100 μ L of MTT solution (5 mg mL⁻¹ in MEM- α) were added and incubated for 4 h in the CO₂ incubator before removal. A hundred microliter of dimethyl sulfoxide was added for dissolving formazan product as produced by live cells. The OD₅₇₀ was measured. The % viability was calculated by comparing with the OD₅₇₀ of the untreated cells that considered as 100% viability.

2.9 Statistical analysis

Each experiment was done in triplicate. Data were expressed as means \pm standard error of the mean (SEM). Student's t-test of IBM SPSS Statistics version 23 was used to evaluate differences between results. The *p*-values of < 0.05 were considered significantly different.

3 Results and Discussion

3.1 XRF spectroscopy

The Zr-HA was synthesized in this study as HA analogue by using wet precipitation method from the stringent mole ratios of Ca(NO₃)₂, (NH₄)₂HPO₄ and ZrO₂ at 65°C and characterized by using XRF and XRD spectroscopy. These techniques are non-destructive and often used for analysis of major or trace elements in rocks, minerals, and sediment. Of the former technique, a set of characteristic fluorescent peaks are emitted after a compound has been excited by bombardment with high-energy X-rays or gamma rays of XRF spectrometer⁽¹⁵⁾. Concentrations in % mole of Ca, P, Zr and others that would present in the Zr-HA samples were quantified and the Ca/P ratios were calculated. The results were shown in Table ?? and Table 2, respectively. The Ca/P ratio of 1.67 has been theoretically assigned to the perfectly stoichiometric HA crystal⁽¹⁶⁾. Instead, the Ca/P ratio of 2.45 was accounted for a HA sample purchased from Sigma-Aldrich. In accordance, this commercialized HA was considered structurally defective and non-stoichiometric although product specification concerning XRD result has indicated it as hydroxyapatite. For the recently synthesized compounds, namely HA, 0.1Zr-HA and 0.5Zr-HA, the Ca/P ratios of 2.67, 2.62 and 2.59 were respectively apparent. Then, the crystal structures of these materials were determined to be highly non-stoichiometric compared to the bought HA. Moreover, substitution of Zr⁴⁺ ions (as dissolved from ZrO₂) in Ca²⁺ lattices of HA possibly occurred although the ionic radius of Zr⁴⁺ ion is significantly longer than that of Ca²⁺ ion (~13.5 Å and ~11.4 Å, respectively)⁽¹⁷⁾. The magnitude of Ca²⁺-Zr⁴⁺ replacement was enhanced in response to an amount of ZrO₂ increasingly added from 0.1 mole to 0.5 mole. Therefore, the lowered crystallinity of 0.5Zr-HA was implicated by comparing with that of 0.1Zr-HA and the synthesized HA. Whether the difference in the crystallinity would have a consequence on the degradability was then

to be clarified⁽¹⁸⁾.

Table 1. Concentrations in % mole of H, C, N, O, Ca, P, and Zr in 0.1Zr-HA and 0.5Zr-HA, determined by XRF spectrometer

| Sample | Concentration (% mole) | | | | | | | | |
|----------|------------------------|-------|-------|--------|--------|--------|-------|----|----|
| | H | C | O | Ca | Zr | Si | Fe | | |
| 0.1Zr-HA | 0.009 | 0.106 | 0.123 | 39.042 | 43.270 | 16.487 | 0.963 | << | << |
| 0.5Zr-HA | 0.019 | 0.230 | 0.269 | 38.412 | 40.565 | 15.649 | 4.857 | << | << |

<<: less than the limit of detection

Table 2. The calculated Ca/P ratios and the % mole of Zr as detected by XRF spectrometer

| Sample | Ca/P ratio | Zr (% mole) |
|--------------------|------------|-------------|
| HA (theoretical) | 1.67 | - |
| HA (Fluka) | 2.45 | Not found |
| The synthesized HA | 2.67 | Not found |
| 0.1Zr-HA | 2.62 | 0.963 |
| 0.5Zr-HA | 2.59 | 4.857 |

3.2 FTIR spectroscopy and rheometric analysis of the modified-PCL

Thin film of PCL was prior generated to increase contact surface area for alkaline hydrolysis based on the surface-erosion mechanism⁽¹⁹⁾. NaOH solution of 3 or 5 mole L⁻¹ was separately used for hydrolyzing the PCL film. Two products, respectively called 3M-PCL and 5M-PCL, were acquired. FTIR spectra of the unmodified PCL, 3M-PCL, and 5M-PCL were demonstrated in Figure 1. There were similarities of peaks around 850-400 cm⁻¹. Thus, the basic ϵ -caprolactone units were commonly present in all tested polymers. Cutting the aliphatic ester bonds of PCL by this strong base was productive, resulting in fragmented PCL polymer that would be different in the numbers of the ϵ -caprolactone units depending on factors such as the base concentration, time duration of contact, as well as surface area of contact⁽²⁰⁾. Of these samples, peaks around 3600-2500 cm⁻¹, 1750-1680 cm⁻¹, and 1460-1380 cm⁻¹ were also coherent, corresponding to carboxylic acid O-H stretching, carboxylic acids and esters C=O stretching, and *sp*³ C-H stretching, respectively. The most intense peaks were noticeable for 5M-PCL. The peaks with moderate %T were revealed by 3M-PCL, and those with the weakest %T were apparent for the unmodified PCL. Presumably, 5M-PCL sample was constituted by the most shortened PCL fragments with the least numbers of the ϵ -caprolactone units of the fragments compared to 3M-PCL and the parent PCL counterparts⁽²¹⁾. It was possible to increase the magnitude of PCL fragmentation by using the more concentrated alkaline solution⁽²²⁾. The viscosity of 50% w/v solutions of the parent PCL, 3M-PCL, or 5M-PCL were determined to be 185.90, 165.27, or 124.73 centipoise (cP), respectively [Table 3]. Again, there was consistency between FTIR result and that of the viscosity. To this regard, PCL was greatly fragmented by using 5 mole L⁻¹ NaOH compared to the 3M concentration, leading to an extensive reduction of the viscosity with the existence of very strong pecks corresponding to O-H and C=O stretching of 5M-PCL. Consequently, 5M-PCL was suggested to have greater hydrophilicity than 3M-PCL.

Table 3. The viscosity of 50% w/v solution in chloroform of the unmodified PCL, 3M-PCL and 5M-PCL

| Sample | Viscosity (cP) |
|----------------|----------------|
| Unmodified-PCL | 185.90±0.30 |
| 3M-PCL | 165.27±0.70 |
| 5M-PCL | 124.73±0.11 |

3.3 XRD spectroscopy and *in vitro* degradation

In the subsequent experiment, 0.5Zr-HA and 5M-PCL were physically mixed at 1:2 and 2:1 w/w ratios to produce porous grains. The diameter of the grains was approximately 2-5 μ m independent of the mixed weight ratio (Figure 2 insert). XRD plots were

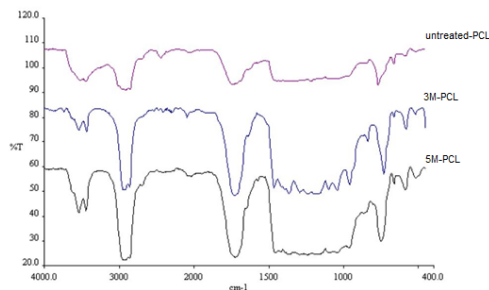


Fig 1. FTIR spectra of the untreated PCL, 3M-PCL, and 5M-PCL; The alkaline treatment was carried out for 6 h at room temperature.

shown in Figure 2. The diffraction of 5M-PCL was insignificantly apparent at $2\theta = 21.320^\circ$, 23.678° , 25.709° , and 28.185° (22). Instead, there were characteristic diffraction peaks of HA at $2\theta = 22.902^\circ$, 46.711° , 48.103° , and 53.143° ; monoclinic zirconium at $2\theta = 24.052^\circ$, 28.172° , and 54.062° ; tetragonal zirconium at $2\theta = 30.262^\circ$, 50.372° , and 60.202° ; octa-calcium phosphate at $2\theta = 31.662^\circ$; amorphous calcium phosphate at $2\theta = 40.862^\circ$; and dicalcium phosphate anhydrate at $2\theta = 22.032^\circ$, 45.402° and 51.530° . The relatively weak diffraction at $2\theta = 22.032^\circ$ and 46.711° became significant as the amount of 0.5Zr-HA increased in the 2:1 w/w composite. Octa-calcium phosphate, amorphous calcium phosphate, and dicalcium phosphate anhydrate were formed as secondary phases in addition to monoclinic zirconium. This monoclinic phase of zirconium has been stable at temperatures below 1170°C (23) and was predicted to present as a major phase in the synthesized Zr-HA after it was sintered at 1150°C . Due to the deformed prism of the monoclinic zirconium, its presence could be disruptive for the Zr-HA precipitation that led to the formation of various calcium phosphate compounds. To our knowledge, the lattice centers of $\text{Rb}^+/\text{Se}^{2+}$ doped HA have been destabilized, and this has rendered it greatly degraded (22). Based on the XRF and XRD results, 0.5Zr-HA was implicated to be more structurally defective and non-stoichiometric than 0.1Zr-HA, the synthesized HA, as well as the brought HA. That the structural integrity of Zr-HA ceramics would affect their degradation was proved after immersed in PBS at 37°C for 8 weeks. Graphs of % weight loss as a function of soaking time periods were shown in Figure 3.

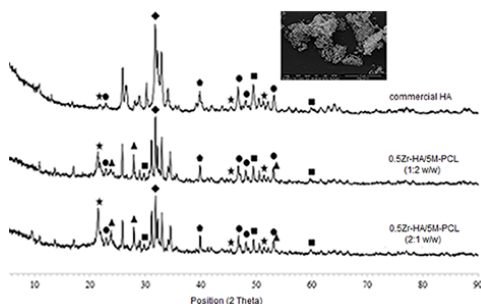


Fig 2. XRD diffractograms of the commercial HA and composites of 1:2 w/w 0.5Zr-HA/5M-PCL and 2:1 w/w 0.5Zr-HA/5M-PCL; the 2θ of HA (circle) at 22.902° , 46.711° , 48.103° , and 53.143° ; the 2θ of monoclinic zirconium (triangle) at 24.052° , 28.172° , and 54.062° ; the 2θ of tetragonal zirconium (square) at 30.262° , 50.372° , and 60.202° ; the 2θ of octa-calcium-phosphate (diamond square) at 31.662° ; the 2θ of amorphous calcium-phosphate (pentagon) at 40.862° ; and the 2θ of dicalcium-phosphate-anhydrate (star) at 22.032° , 45.402° and 51.530° ; **Figure 2 insert** SEM micrograph of grains of 0.5Zr-HA/5M-PCL mixtures

Increased degradation was evident for samples containing 5M-PCL compared to those composing of the unmodified-PCL, i.e., 9% and 6% weight loss were corresponded to the 2:1 w/w samples of 0.5Zr-HA/5M-PCL and 0.5Zr-HA/PCL, respectively. Indeed, losing of the % weight was significant for composites that contained greater weight ratio of 0.5Zr-HA, i.e., 0.5Zr-HA/PCL (2:1 w/w) and 0.5Zr-HA/PCL (1:2 w/w) exhibited 7% and 6% weight loss, respectively. In accordance, the ability to absorb water of these mixtures was definitely related to the amounts of 0.1Zr-HA and 0.5Zr-HA therein. As the hydrophilicity of PCL and its modified analogues was arranged in an increased order of $\text{PCL} < 3\text{M-PCL} < 5\text{M-PCL}$, the absorbed water that available was beneficial for inducing degradation of the Zr-HA ceramics and hydrolysis of the polymers to result in significant weight loss (24).

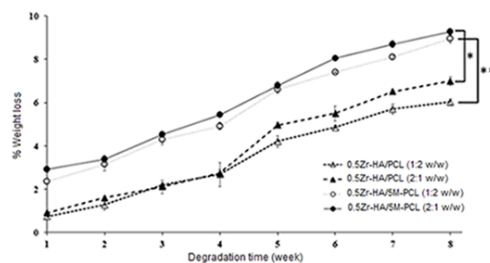


Fig 3. Graphs of % weight loss as a function of times of samples containing 0.5ZrHA/ PCL and 0.5ZrHA/5M-PCL at 1:2 and 2:1 w/w ratios; *, $p < 0.05$; **, $p < 0.01$

3.4 Binding and releasing of TB

TB was used as a model drug to assess binding affinity and release property to and from drug carriers recently prepared. Likely, dipole-dipole, $\pi - \pi$ and charged-charged interactions were mediated in TB binding. In Figure 4, the levels of 13.6%, 17.9%, and 52.6% of the dye were calculated to bind to the 2:1 w/w samples of 0.5Zr-HA/PCL, 0.5Zr-HA/3M-PCL, and 0.5Zr-HA/5M-PCL, respectively. For the 2:1 w/w mixtures containing 0.1Zr-HA/PCL, 0.1Zr-HA/3M-PCL, and 0.1Zr-HA/5M-PCL, the binding of 13.2%, 18.5%, and 48.6% were respectively accounted. It was noticed that the dye would have greater affinity to samples that contained 5M-PCL compared to those of the parent PCL and 3M-PCL. In addition, replacement of 0.1Zr-HA constituent by 0.5Zr-HA counterpart did not affect the TB binding. Presumably, interactions between TB and the unmodified PCL were not sufficiently strong, corresponding to rapid release of the dye from 0.5Zr-HA/PCL specimens after immersed in PBS. Results of TB release test were shown in Figure 5A-C. Clearly, burst release was not detected. Rapid release was apparent within 15 h of the immersion, and gradual release was followed throughout the 120-h time period. Concerning 0.1Zr-HA/PCL and 0.5Zr-HA/PCL composites, the release was maximum at 70%, and the corresponding release profiles were slightly different [Figure 5A]. Superimposition between the release profile of 0.1Zr-HA/3M-PCL sample and that of 0.5Zr-HA/3M-PCL was indicated, reaching the maximum at 60% [Figure 5B]. Additionally, the release profile of 0.1Zr-HA/5M-PCL composite was lined above that of 0.5Zr-HA/5M-PCL specimen and approached the maximum at 40% and 35%, respectively [Figure 5C]. Therefore, TB was relatively preferent in binding to 0.1Zr-HA ceramic compared to 0.5Zr-HA counterpart. In substitution of 3M-PCL by 5M-PCL and the parent PCL by 3M-PCL for the prepared mixtures, again, the dye was highly adherent to those containing 5M-PCL compared to those composing 3M-PCL and the untreated PCL. Taken together, surface hydrophilicity of 0.5Zr-HA/5M-PCL samples were presumably greater than those of 0.5Zr-HA/3M-PCL and 0.5Zr-HA/PCL⁽²⁵⁾, resulting in that the binding of TB on the former carrier system was promoted. Consequently, modification of the hydrophobic/hydrophilic property of any drug carriers was possible, and this would be carried out for obtaining desirable drug loading/releasing characteristics⁽²⁶⁾.

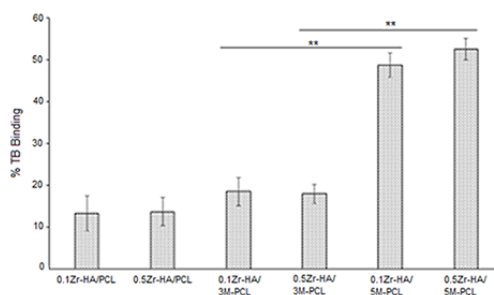


Fig 4. Graphs of % TB binding of composites containing different HA ceramics and PCL or the modified PCL at a 2:1 w/w ratio; **, $p < 0.01$ 5ZrHA/5M-PCL at 1:2 and 2:1 w/w ratios; *, $p < 0.05$; **, $p < 0.01$

3.5 Cytotoxicity testing

MTT method was applied for evaluation of cytotoxicity of the established drug delivery systems using L929 fibroblast cell line. In Figure 6, the % cell viability after challenged with any tested solution for 24 h was not significantly different from that

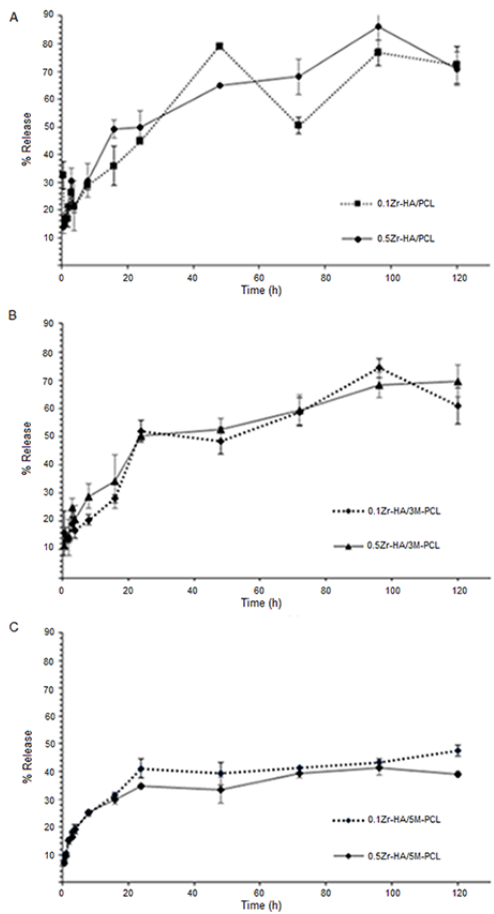


Fig 5. TB release profiles after immersed in PBS for 120 h of composites: (A), 0.1Zr-HA/PCL and 0.5Zr-HA/PCL; (B), 0.1Zr-HA/3M-PCL and 0.5Zr-HA/3M-PCL; and (C), 0.1Zr-HA/5M-PCL and 0.5Zr-HA/5M-PCL, all mixtures were prepared at a 1:2 w/w ratio

of the control. The result suggested that all the recently developed materials were preliminarily noncytotoxic.

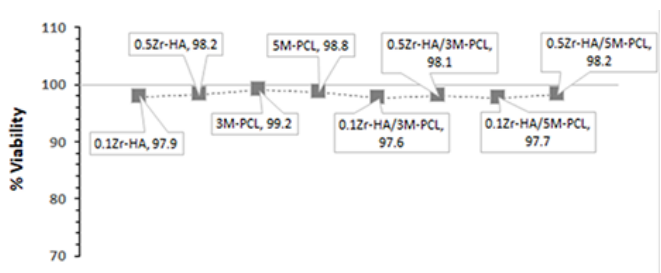


Fig 6. Graphs of % viability of L929 fibroblast cells after treatment for 24 h as determined by MTT method, A sample was immersed in 2 mL PBS for 24 h at room temperature with gentle shaking, and the supernatant was filtered through a 0.22- μ m syringe filter before use in the cytotoxicity testing.

4 Conclusion

HA is one of inorganic materials frequently used to blend with biodegradable polymers for preparation of implants or drug carriers, which to be applied in maxillofacial surgery and restorative dentistry. The *in vitro* degradation of these composites is

controlled by their physicochemical properties and is helpful in prediction of their persistence in oral cavities. To maximize the restoring outcomes, appropriate degradability of any developing materials needs to be tailored *in vitro*. Decreasing the crystallinity of HA by Zr⁴⁺ insertion is another attractive procedure to gain the more non-stoichiometric, highly degradable, and rather porous 0.1Zr-HA and 0.5Zr-HA compared to HA. Increased hydrophilicity of PCL is obtainable by using concentrate NaOH for hydrolysis because hydroxyl functional groups of the fragmented PCL are increasingly existent. The degradability and dye binding affinity of the resulting compound pairs, 0.1Zr-HA/0.5Zr-HA and 3M-PCL/5M-PCL, are superior compared to the unmodified HA and PCL. Preparation of composites containing different weight ratios of Zr-HA and the modified-PCL is valuable for extemporaneous use as drug carriers/fillers in oral cavities of restorative procedures. Increase of the bioavailability of drugs and decrease of drug adverse effects are hopeful with their utilization. Although all the recently prepared materials are non-cytotoxic *in vitro*, other related *in vivo* toxicities, including inflammatory responses are awaited to clarify using rat model.

References

- 1) Wang B, Mastrogiacomo S, Yang F, Shao J, Ong MMA, Chanchareonsook N, et al. Application of BMP-Bone Cement and FGF-Gel on Periodontal Tissue Regeneration in Nonhuman Primates. *Tissue Engineering Part C: Methods*. 2019;25(12):748–756. Available from: <https://doi.org/10.1089/ten.TEC.2019.0160>.
- 2) Parhizkar A, Asgary S. Local Drug Delivery Systems for Vital Pulp Therapy: A New Hope. *International Journal of Biomaterials*. 2021;2021:1–9. Available from: <https://doi.org/10.1155/2021/5584268>.
- 3) Shi P, Liu M, Fan F, Yu C, Lu W, Du M. Characterization of natural hydroxyapatite originated from fish bone and its biocompatibility with osteoblasts. *Materials Science and Engineering C*. 2018;90:706–712. Available from: <https://doi.org/10.1016/j.msec.2018.04.026>.
- 4) Wu VM, Ahmed MK, Mostafa MS, Uskoković V. Empirical and theoretical insights into the structural effects of selenite doping in hydroxyapatite and the ensuing inhibition of osteoclasts. *Materials Science and Engineering C*. 2020;117:111257–111257. Available from: <https://doi.org/10.1016/j.msec.2020.111257>.
- 5) Singh A, Dubey AK. Various Biomaterials and Techniques for Improving Antibacterial Response. *ACS Applied Bio Materials*. 2018;1(1):3–20. Available from: <https://doi.org/10.1021/acsabm.8b00033>.
- 6) Moradi KH, Alvani AAS. First-principles study on Sr-doped hydroxyapatite as a biocompatible filler for photo-cured dental composites. *Journal of the Australian Ceramic Society*. 2020;56(2):591–598. Available from: <https://doi.org/10.1007/s41779-019-00369-9>.
- 7) d'Avanzo, Bruno MC, Giudice A, Mancuso A, Gaetano F, Cristiano MC, et al. Influence of materials properties on bio-physical features and effectiveness of 3D-scaffolds for periodontal regeneration. *Molecules*. 2021;26(6). Available from: <https://doi.org/10.3390/molecules26061643>.
- 8) Halim A, Hussein NA, Kandar MZ, K M. Nanomaterials-Upconverted Hydroxyapatite for Bone Tissue Engineering and a Platform for Drug Delivery. *International Journal of Nanomedicine*. 2021;16:6477–6496. Available from: <https://doi.org/10.2147/IJN.S298936>.
- 9) Simone S, Massimiliano D, Lorenzo P, Elisa M, Rosa MI, Fernanda M, et al. Enhancement of the biological and mechanical performances of sintered hydroxyapatite by multiple ions doping. *Frontier Materials*. 2020;7:224–224. Available from: <https://doi.org/10.3389/fmats.2020.00224>.
- 10) Park J, Kim BJJ, Hwang JYY, Yoon YWW, Cho HSS, Kim DHJ, et al. In-Vitro Mechanical Performance Study of Biodegradable Polylactic Acid/Hydroxyapatite Nanocomposites for Fixation Medical Devices. *Journal of Nanoscience and Nanotechnology*. 2018;18(2):837–841. Available from: <https://doi.org/10.1166/jnn.2018.14884>.
- 11) Jiao Z, Luo B, Xiang S, Ma H, Yu Y, Yang W. 3D printing of HA / PCL composite tissue engineering scaffolds. *Advanced Industrial and Engineering Polymer Research*. 2019;2(4):196–202. Available from: <https://doi.org/10.1016/j.aiepr.2019.09.003>.
- 12) Colmenares G, Agudelo-Gomez ML, Pinal R, Hoyos-Palacio L. Production of bioabsorbible nanoparticles of polycaprolactone by using a tubular recirculating system. *Dyna (Medellin, Colombia)*. 0204;p. 85–85. Available from: <https://doi.org/10.15446/dyna.v85n204.62292>.
- 13) Thanyaphoo S, Kaewsrichan J. A new biocompatible delivery scaffold containing heparin and bone morphogenetic protein 2. *Acta Pharm*. 2016;66(3):373–85. Available from: <https://doi.org/10.1515/acph-2016-0026>.
- 14) Manee S, Kaewsrichan J. Cosmeceutical Benefit of *Abelmoschus esculentus* L. Seed Extract. *Journal of Pharmaceutical Research International*. 2017;19(6):1–11. Available from: <https://doi.org/10.9734/JPRI/2017/37587>.
- 15) Sabri MM. Chemical and Structural Analysis of Rocks Using X-ray Fluorescence and X-ray Diffraction Techniques. *ARO-The Scientific Journal of Koya University*. 2020;8(1):79–87. Available from: <https://doi.org/10.14500/aro.10643>.
- 16) Iviglia G, Kargozar S, Baino F. Biomaterials, Current Strategies, and Novel Nano-Technological Approaches for Periodontal Regeneration. *Journal of Functional Biomaterials*. 2019;10(1):3–3. Available from: <https://doi.org/10.3390/jfb10010003>.
- 17) Periodic Trends . 2021. Available from: https://www.lamar.edu/arts-sciences/_files/documents/chemistry-biochemistry/dorris/chapter7.pdf.
- 18) Gomez-Vazquez OM, Correa-Piña BA, Zubieta-Otero LF, Castillo-Paz AM, Londoño-Restrepo SM, Rodríguez-García ME. Synthesis and characterization of bioinspired nano-hydroxyapatite by wet chemical precipitation. *Ceramics International*. 2021;47(23):32775–32785. Available from: <https://doi.org/10.1016/j.ceramint.2021.08.174>.
- 19) Rubí-Sans G, Recha-Sancho L, Pérez-Amodio S, Ángel Mateos-Timoneda M, Semino CE, Engel E. Development of a Three-Dimensional Bioengineered Platform for Articular Cartilage Regeneration. *Biomolecules*. 2019;10(1):52–52. Available from: <https://doi.org/10.3390/biom10010052>.
- 20) Guo N. Preparation and degradation behavior of polycaprolactone nano-porous membrane. *CMULJ*. 2018;45(7):2790–2796. Available from: <http://cmuir.cmu.ac.th/jspui/handle/6653943832/64246>.
- 21) Ren J, Kohli N, Sharma V, Shakouri T, Keskin-Erdogan Z, Saifzadeh S, et al. Poly-ε-Caprolactone/Fibrin-Alginate Scaffold: A New Pro-Angiogenic Composite Biomaterial for the Treatment of Bone Defects. *Polymers*. 2021;13(19):3399–3399. Available from: <https://doi.org/10.3390/polym13193399>.
- 22) Ahmed MK, Al-Wafi R, Mansour SE, El-Dek SI, Uskoković V. Physical and biological changes associated with the doping of carbonated hydroxyapatite/polycaprolactone core-shell nanofibers dually, with rubidium and selenite. *Journal of Materials Research and Technology*. 2020;9(3):3710–3723. Available from: <https://doi.org/10.1016/j.jmrt.2020.01.108>.
- 23) Bapat RA, Yang HJ, Chahal TV, Dharmadhikari S, Abdulla AM, Arora S, et al. Review on synthesis, properties and multifarious therapeutic applications of nanostructured zirconia in dentistry. *RSC Advances*. 2022;12(20):12773–12793. Available from: <https://doi.org/10.1039/d2ra00006g>.

- 24) Raju G, Haris MRHM, Azura AR, Eid AMAM. Chitosan Epoxidized Natural Rubber Biocomposites for Sorption and Biodegradability Studies. *ACS Omega*. 2020;5(44):28760–28766. Available from: <https://doi.org/10.1021/acsomega.0c04081>.
- 25) Rohiwal SS, Ellederová Z, Ardan T, Klima J. Advancement in Nanostructure-Based Tissue-Engineered Biomaterials for Retinal Degenerative Diseases. *Biomedicines*. 2021;9(8):1005–1005. Available from: <https://doi.org/10.3390/biomedicines9081005>.
- 26) Yarce CJ, Echeverri JD, Salamanca CH. Effect of the Surface Hydrophobicity Degree on the In Vitro Release of Polar and Non-Polar Drugs from Polyelectrolyte Matrix Tablets. *Polymers*. 2018;10(12):1313–1313. Available from: <https://doi.org/10.3390/polym10121313>.